IEEE Access
Multidisciplinary ⋮ Rapid Review ⋮ Open Access Journal

Received September 2, 2020, accepted September 12, 2020, date of publication September 18, 2020, date of current version September 30, 2020.

Digital Object Identifier 10.1109/ACCESS.2020.3024828

Residual Flux Density Measurement Method of Single-Phase Transformer Core Based on Time Constant

CAILING HUO, SHIPU WU, YIMING YANG, CHENGCHENG LIU, (Member, IEEE), AND YOUHUA WANG

State Key Laboratory of Reliability and Intelligence of Electrical Equipment, Hebei University of Technology, Tianjin 300130, China
Key Laboratory of Electromagnetic Field and Electrical Apparatus Reliability of Hebei Province, Hebei University of Technology, Tianjin 300130, China

Corresponding author: Youhua Wang (wangyi@hebut.edu.cn)

This work was supported in part by the National Natural Science Foundation of China under Grant 51877065.

ABSTRACT Residual flux density in the single-phase transformer core can dramatically increase inrush current when the transformer is energized. To reduce inrush current, it is necessary to study residual flux density measurement. This paper proposes a new residual flux density measurement method based on time constant. Firstly, the generation principle of residual flux density is analyzed under different magnetization states, and it is found that the positive relative differential permeability is smaller than the negative at different residual flux density. To obtain the relative differential permeability, when an appropriate DC excitation is applied, the measurement circuit is equivalent to a first-order RL circuit. Then, combining magnetic circuit and transient circuit analysis, the relationship between time constant and relative differential permeability is obtained. It is conclusion that the positive time constant is less than the negative. Residual flux density direction is determined by comparing the positive and negative time constant, and the magnitude of residual flux density is calculated by the relationship between residual flux density and the difference of the positive and negative time constant. Finally, the empirical formula between residual flux density and time constant difference of the square core is obtained in finite element method, and then verified on the experimental platform. Compared with other measurement methods, the relative error of proposed empirical formula is within 4.58 %, and it has higher accuracy in this paper. The proposed method in this paper can provide a reference for selecting the demagnetization voltage, which improves the effectiveness of demagnetization.

INDEX TERMS Residual flux density, relative differential permeability, time constant difference, empirical formula.

I. INTRODUCTION

When the power transformer is cut-out operation and in various test operations [1]–[3], the internal magnetic flux density in the iron core does not fall to zero and thus an unknown residual flux density (B_r) is produced, which is resulted by the hysteresis characteristics of iron core materials [4]–[6]. When the transformer is switched to connect with power grid again, a magnetizing inrush current will be produced as the existence of B_r [7], [8]. Sometimes this current may be 6 to 8 times higher than the rated state current [9], which will result the transformer failing to connect with the power grid. To suppress inrush current, synchronous closing technology and phase selection closing technology are proposed in [10]–[12], on the premise of B_r magnitude and direction being obtained [13]. Moreover, demagnetization without knowing the magnitude of B_r in the transformer core is not only time consuming and laborious, but also has a poor demagnetization effect [14]. Thus, it is of great significance to accurately detect B_r in the transformer core for the safe operation of large power transformers and even power grids.

At present, there are five main methods for measuring the B_r in the transformer core:

1) Estimation method. When large power transformers leave the factory, empirical estimation method is generally used to estimate B_r in the iron core. And, it is considered that B_r is 20 % - 80 % of the saturated flux density [15]. In [16], B_r is found not to higher than 0.7 times of the saturated flux

The associate editor coordinating the review of this manuscript and approving it for publication was Giambattista Gruosso.

This work is licensed under a Creative Commons Attribution-NonCommercial-NoDerivatives 4.0 License.
For more information, see https://creativecommons.org/licenses/by-nc-nd/4.0/

density by analyzing more than 500 transformers. However, this method can only roughly estimate the range of B_r and cannot accurately predict the magnitude of B_r in the iron core.

2) Indirect measurement method. In [17], the B_r before energization is calculated based on the obtained peak value of the magnetizing inrush current after the transformer is energized. However, it is not sure that this method can be applied to B_r measurement before the transformer is closed.

3) Pre-magnetization method. By applying larger current to the core, the internal flux density of the core is changed from original B_r to saturated magnetic flux density. After that the phase selection closing technology or demagnetization method is used to suppress the magnetizing inrush current [18]–[20]. In [21], the DC voltage excitation with varying polarity to measure B_r is proposed, which is essentially the same as the pre-magnetization method. Although the magnitude of B_r can be measured, the B_r has been changed to saturated flux density, and a large current to saturate the iron core is required. Finally, for demagnetizing B_r, the extra time and expensive equipment are required.

4) Voltage integration method. This method is based on the electromagnetic induction law [22], [23]. By recording the voltage waveform at the transformer opening time, the B_r is obtained by the voltage integration method. However, the upper limit of the integration (the time of opening) is not easily determined. Due to hysteresis characteristics of the ferromagnetic material, measured B_r at the moment of opening is different from B_r after stabilization and thus the feasibility of this method is limited.

5) Transient excitation measurement method. In [24], the B_r is obtained by establishing the relationship between B_r and magnetizing current. However, this method uses the magnetization curve in the simulation model, thus this accuracy is greatly reduced and the B_r direction is not judged. To address the limitations of this approach, in [25], author analyzes the relationship between B_r and transient current difference. However, the measurement time of transient current difference is not easily determined, which may result in a lower accuracy of calculated B_r. In [26], the B_r is calculated based on the positive time constant. However, the B_r is only measured in known B_r directions, and not in unknown directions. Moreover, the influence of external excitation on B_r is not analyzed. Therefore, there is no effective method for measurement B_r in the iron core.

To accurately measure B_r in the iron core, this paper proposes a new B_r measurement method. This method has several improvements over the above methods as follows:

1) The relationship between B_r, the difference of the positive and negative time constant, and external DC voltage is theoretically analyzed. Then, the square iron core is taken as the research object, and the empirical formula for measuring B_r is obtained by finite element method (FEM).

2) Through analysis the relationship between the relative differential permeability (μ_{rd}) and the corresponding time constant at B_r, the B_r direction is determined.

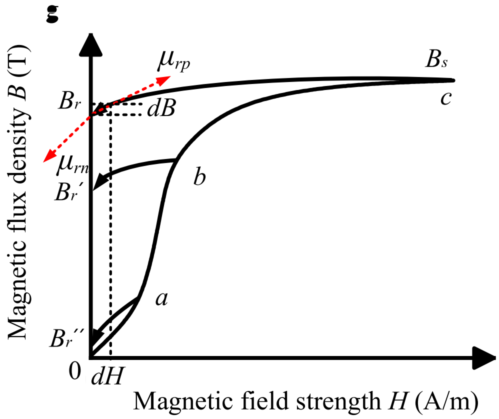

FIGURE 1. The generation principle of B_r in the iron core under different magnetization states.

3) Through numerical simulation analysis, the range of applied DC excitation is analyzed and determined. Then the B_r test platform of the square core is established to verify the accuracy of proposed method. Experimental results prove that the B_r measurement method proposed in this paper has higher accuracy compared with existing methods.

The rest of the paper is organized as follows. The basic principle of proposed B_r measurement method is analyzed in Section II. Section III obtains the proposed empirical formula of the square iron core in FEM. In Section IV, the accuracy of proposed empirical formula and the feasibility of proposed B_r measurement method are verified in the square iron core test platform. Section V concludes the paper.

II. PRINCIPLE OF PROPOSED RESIDUAL FLUX DENSITY MEASUREMENT METHOD

A. GENERATION PRINCIPLE OF RESIDUAL FLUX DENSITY

When the transformer core is externally excited, due to the magnetic domain structure changes inside the core material, the ferromagnet exhibits certain magnetic properties to the outside [27]. Fig. 1 shows B_r generation principle under different magnetization states. As shown, the magnetization process is divided into three states: 1) Reversible magnetization state. When the external magnetic field strength (H) increases from 0 to point a, the magnetic domains change will occur in reversible magnetization stage. And then when H disappears, $B_{r''}$ is almost not generated. 2) Irreversible magnetization state. As H increases to point b, the magnetic domains movement begins to change from reversible magnetic domain wall displacement to irreversible magnetic domain wall displacement, thereby exhibiting stronger magnetism to the outside world. When H suddenly disappears, the magnetic domain state cannot be restored to the original state, but formed a new state, which results in a phase difference between B and H, which is called hysteresis. At this time, $B_{r'}$ in the iron core cannot be ignored. 3) Saturated magnetization state. When H continues to increase to point c, the magnetic domain movement enters the saturated state. After H disappears, a large B_r is generated and is not ignored.

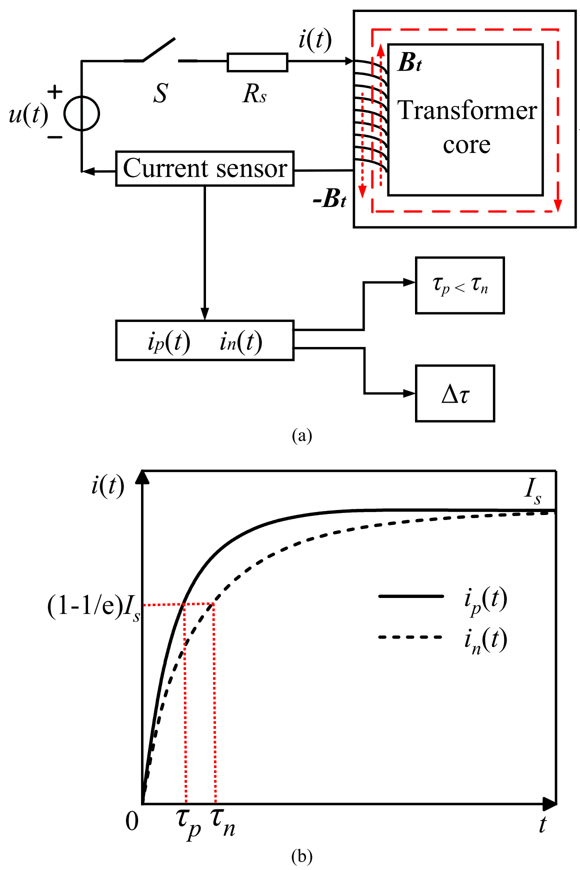

FIGURE 2. The basic principle of proposed B_r measurement method in this paper, (a) the measurement circuit of the proposed method and (b) the positive and negative transient current waveforms.

B. PROPOSED RESIDUAL FLUX DENSITY MEASUREMENT METHOD

The square iron core is selected as the research object in this paper. Fig. 2 shows the basic principle of proposed B_r measurement method. As shown in Fig. 2(a), the measurement circuit of proposed method is presented. B_r is the initial residual flux density in the iron core determined by a large current. The DC voltage $u(t)$ is applied to the measuring winding to exaction a test flux density (B_t) on initial B_r. When a positive DC voltage with the same polarity is applied, B_t is generated on the basis of the initial B_r so that the actual B_r in the iron core will increase. In addition, when using a negative DC voltage with the opposite polarity to B_r, -B_t is generated on the initial B_r and the magnitude of B_r will decrease. At the same time, corresponding transient current $i(t)$ is generated, as shown in Fig. 2(b).

When a positive DC voltage is applied in the measuring winding, the positive transient current $i_p(t)$ increases. While a negative DC voltage with the opposite polarity to B_r is applied, the negative transient current $i_n(t)$ will be decreased. However, compared to the first process, due to the hysteresis phenomenon of the iron material, the change rate of $i_p(t)$ is slower than $i_n(t)$ (see Fig. 2 (b)). The change rate of $i_p(t)$ or $i_n(t)$ is reflected by the positive or negative time constant (τ_p or τ_n) in the transient process. Time constant is defined as this moment when the steady-state value I_s of the transient current drops 1/e. Thus, the direction of B_r is determined by comparing τ_p and τ_n, and the relationship between B_r and the difference $\Delta\tau$ of τ_p and τ_n is found to determine the magnitude of B_r in the iron core. $\Delta\tau$ at B_r is expressed as

$$\Delta\tau = \left|\tau_p - \tau_n\right| \tag{1}$$

According to above analysis, the proposed relationship for calculating B_r in the iron core is expressed as

$$B_r = f\,(\Delta\tau) \tag{2}$$

This method also considers the influence of different external DC voltage (It is also the applied B_t value) on B_r in the iron core. To ensure higher accuracy of proposed measurement method, when the DC voltage is applied, it is acceptable to keep the change rate of B_r is within 10 %. In the following sections, this relationship will be obtained by FEM and verified by experiments.

C. DETERMINING DIRECTION OF RESIDUAL FLUX DENSITY

Due to the hysteresis phenomenon of the ferromagnetic material, its magnetization state cannot be restored to the magnetic neutral state, but maintains the B_r state. Therefore, the B_r depends mainly on the magnetic domain structure change from maximum flux density state to B_r state, which is reflected by the change of the relative differential permeability (μ_{rd}) at B_r [26]. As shown in Fig. 1, μ_{rd} at B_r is defined as the ratio of magnetic flux density increment dB and magnetic field strength increment dH.

$$\mu_{rd} = \frac{1}{\mu_0}\frac{dB}{dH} \tag{3}$$

When H changes from positive to negative in the vicinity of B_r, the magnetization ability of magnetic domain increases from small to large and thus μ_{rd} at B_r also increases from small to large, as shown in Fig. 1. The relationship between positive and negative relative differential permeability (μ_{rp} and μ_{rn}) at B_r is as follows:

$$\mu_{rp} < \mu_{rn} \tag{4}$$

Based on the magnetic circuit analysis [25], the relationship between the equivalent inductance L_{eq} and μ_{rd} at B_r is expressed as

$$L_{eq} = \frac{N^2 S\mu_0}{l}\mu_{rd} \tag{5}$$

where N expresses the ratio of measuring winding, S and l represent the cross-sectional area and the average magnetic path length of the iron core, respectively. μ_0 expresses the vacuum permeability of air, and its value is $4\pi \times 10^{-7}$ H/m.

When the DC voltage is applied, the measurement circuit is modeled as a RL parallel equivalent circuit, as shown in Fig. 3. As shown, R_s includes the internal source resistance,

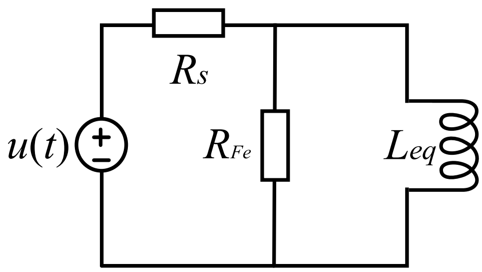

FIGURE 3. The equivalent circuit when the DC excitation is applied.

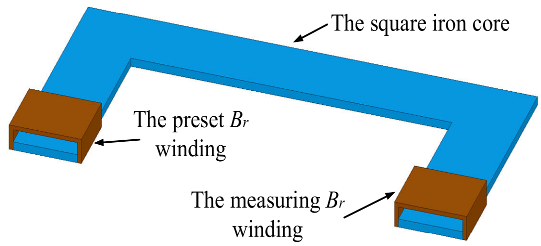

FIGURE 4. The square iron core model set in FEM.

connecting wires resistance, and winding resistance. L_{eq} represents equivalent magnetized inductance of measuring winding, which is effect by the magnetic flux in the iron core. R_{Fe} expresses the iron loss resistance. When the appropriate DC voltage is applied, the change rate of B_r in the iron core is within 10 %. At this time, resistance R_{Fe} can be ignored in the transient progress.

When the external DC voltage is applied, the time constant τ in the circuit is described as:

$$\tau = \frac{L_{eq}}{R} \tag{6}$$

where R expresses the total resistance in the circuit. According to (5) and (6), the relationship between τ and μ_{rd} at B_r is expressed as

$$\tau = \frac{N^2 S\mu_0}{Rl}\mu_{rd} \tag{7}$$

It can be seen that the changes of μ_{rp} and μ_{rn} at B_r can be directly reflected by τ_p and τ_n in the transient circuit. Based on (4) and (7), the relationship between τ_p and τ_n at B_r is expressed as

$$\tau_p < \tau_n \tag{8}$$

Thus, the direction of B_r is determined by comparing τ_p and τ_n at B_r when the appropriate DC voltage is applied.

III. PARAMETERS DETERMINATION AND SIMULATION ANALYSIS

In this paper, an experiment platform which adopts square stacked steel sample is built, as shown in Fig. 12. The main dimension of the iron core is determined as the S = 0.0016 m^2, l = 1.92 m. Fig. 4 shows the square iron core model in FEM. As shown, the turns of preset B_r winding are 50, and the turns of measuring winding are 10. Before the numerical simulation analysis, it is necessary to discuss the range of preset B_r and the selection of external DC excitation.

A. RANGE OF RESIDUAL FLUX DENSITY

When the measurement frequency is 5 Hz, the magnetization curve of stacked steel sample is obtained, as shown in Fig. 5. As shown, the saturated flux density of the iron core material can reach 1.8 T. According to the empirical estimation method [15], [16], the B_r is 20 % -70 % of the saturated flux density in the iron core. Thus, the range of preset B_r is 0.36 T-1.26 T in the simulation and experiments. Preset B_r values selected in this paper are shown in TABLE 1.

TABLE 1. Preset residual flux density values.

B_{r1}/T	B_{r2}/T	B_{r3}/T	B_{r4}/T	B_{r5}/T	B_{r6}/T	B_{r7}/T	B_{r8}/T
0.44	0.68	0.76	0.83	0.97	1.02	1.08	1.18

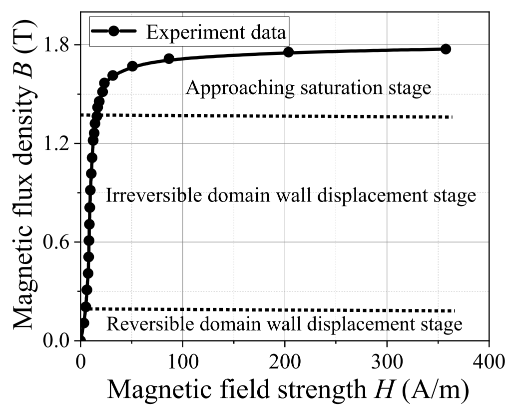

FIGURE 5. The magnetization curve of steel sample at measurement frequency is 5 Hz.

B. SELECTION OF EXTERNAL DC EXCITATION

When B_r is zero, B_t value is determined by applying DC voltage. Then, when B_r is not zero, DC voltages of the same magnitude and different directions are loaded. Due to the hysteresis effect of the iron core, the change of B_r is smaller than the actual applied B_t value. Moreover, when applied B_t value is larger, the change of initial B_r becomes larger. To improve the measurement accuracy, the applied DC voltage cannot make the change rate of initial B_r exceed 10 %.

As shown in Fig. 5, the overall magnetization curve is divided into three stages: 1) In the stage of reversible magnetic domain wall displacement. The maximum flux density in the iron core can approximately reach 0.2 T. When H disappears, the magnetization can return to the original state along the original path. At this time, B_r is close to zero. 2) In the stage of irreversible magnetic domain wall displacement. When H disappears, the magnetization cannot be restored to the original magnetization state, but there is a phase difference between B and H, resulting in hysteresis.

At this time, B_r cannot be ignored. 3) In the approaching the saturation stage. Hysteresis phenomenon is more obvious than the previous two stages. When H disappears, generated B_r is too large to be ignored. When the applied B_t is greater than the flux density in the reversible magnetic domain wall displacement stage, the change of initial B_r is larger affected. Therefore, the applied B_t value is not larger than 0.2 T. At this time, the relationship between B and H is almost linear, as shown in Fig. 5. The applied B_t is expressed as

$$B_t = \mu H \tag{9}$$

where the permeability μ is obtained by the data fitting and its value is 0.05 H/m.

According to the ampere loop law, the above equation is obtained:

$$\frac{u(t)}{R} \cdot N = H \cdot l \tag{10}$$

where N expresses the turns of the measuring winding and its value is 10. R expresses the total resistance in the measurement circuit and its value is 5.04 Ω.

According to (9) and (10), the external DC voltage $u(t)$ can be obtained.

$$u(t) = \frac{Rl}{\mu N} B_t \tag{11}$$

When a positive or negative DC voltage is applied, due to the hysteresis characteristics of core material, B_r in the iron core is changed from initial B_r to new B_{r1} or B_{r2}. The change ΔB of flux density is different in the positive and negative directions. To describe the effect of external excitation on B_r, the change rate B_r % of B_r is defined as

$$B_r\% = \left| \frac{\Delta B}{B_r} \right| \times 100\% \tag{12}$$

where the positive ΔB is expressed by B_{r1} - B_r, and the negative ΔB is expressed by B_{r2} - B_r.

Fig. 6 shows the change of B_r % under different B_t when B_r is 0.83 T. As shown, the positive B_{r1} % and negative B_{r2} % increase as applied B_t value increases. Since the change of μ_{rp} at B_r is smaller than μ_{rn}, the magnetization ability in the positive direction is weaker than that of the negative, and thus B_{r1} % is less than B_{r2} %. When - B_t is applied, the variation of B_r % is greater than that with the positive. Therefore, when B_{r2} % is less than 10 %, the maximum value of B_t is determined.

Fig. 7 shows the change of B_r % under different B_r and different B_t. As shown, as B_r increases, corresponding B_{r1} % and B_{r2} % gradually become smaller. And, B_{r2} % is less than 10 % under the situations: 1) when B_t is less than 0.10 T, corresponding B_{r2} % is less than 10 % in the range of preset B_r and 2) when B_t is larger than 0.10 T and less than 0.15 T, corresponding B_{r2} % is less than 10 % at B_r >1.0 T. The above two situations can meet the conditions of B_t selection. Thus, B_t value is selected in the range of 0.15 T.

At the same time, when the positive and negative B_t are applied, τ_p and τ_n are obtained by corresponding transient

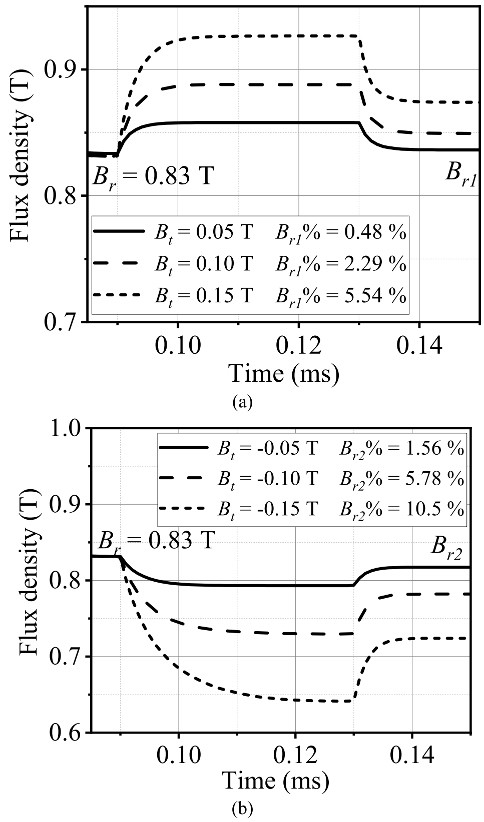

FIGURE 6. The change of B_r % under different B_t when B_r is 0.83 T, (a) the change of B_{r1} % and (b) the change of B_{r2} %.

TABLE 2. Applied test flux density and DC voltage value.

B_t/T	0.05	0.10	0.15
$u(t)$/V	1.00	2.00	3.00

current. When applied B_t value is 0.05 T, 0.1 T and 0.15 T, the changes of τ_p and τ_n are shown in Fig. 8. It can be seen that corresponding $\Delta\tau$ is more and more obvious as B_r increases. When B_t = 0.05 T and preset B_r < 0.44 T, τ_p is close to τ_n and thus corresponding $\Delta\tau$ is almost to zero. At this time, the direction of B_r in the iron core is not easily determined. To make the direction of B_r can be accurately judged, the applied B_t value is not less than 0.05 T. Based on the above analysis, applied B_t value varies within the range of 0.05 T - 0.15 T, and then corresponding $u(t)$ is obtained by equation (11), as shown in TABLE 2.

C. EMPIRICAL FORMULA FOR CALCULATING RESIDUAL FLUX DENSITY

Fig. 9 shows the $i_p(t)$ and $i_n(t)$ waveforms when B_t is 0.1 T and B_r is 0.83 T. As shown, τ_p and τ_n can be obtained by $i_p(t)$ and $i_n(t)$ waveforms. The time constant is mainly affected by the equivalent inductance value in the equivalent circuit, which is related to μ_{rd} at B_r. When the positive and negative B_t is applied, as B_r increases, the change of μ_{rp} is smaller than μ_{rn}. Thus, τ_p is less than τ_n at different B_r. By comparing τ_p and τ_n, the direction of B_r in the iron core is determined.

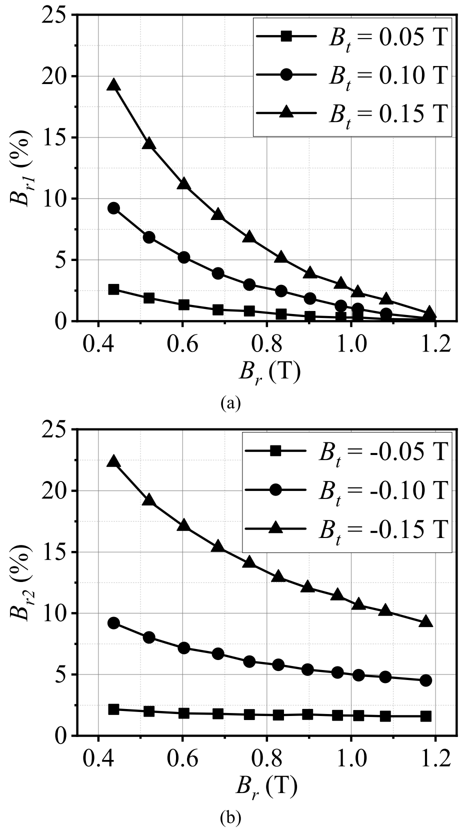

FIGURE 7. The change of B_r % under different B_r and different B_t, (a) the change of B_{r1} % and (b) the change of B_{r2} %.

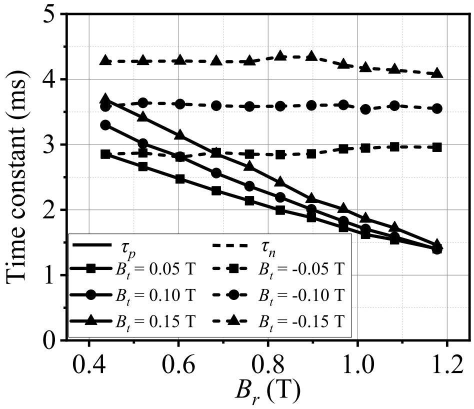

FIGURE 8. The change of the τ_p and τ_n at different B_r when the B_t is 0.05 T, 0.10 T and 0.15 T.

After determining B_r direction in the iron core, to obtain the empirical formula of square iron core, the relationship between B_r and $\Delta\tau$ at different B_r and different B_t is analyzed. When B_t is 0.1 T and -0.1 T, the $i_p(t)$ and $i_n(t)$ waveforms and corresponding time constant changes are shown in Fig. 10(a) and Fig. 10(b). It can be seen that τ_p or τ_n is obtained by corresponding transient current waveforms (see Fig. 10(c)). As shown in Fig. 10(c), the change of τ_p linearly decreases as B_r increases, which is greatly affected by B_r in the iron core. While the change of τ_n is slow with the increase of B_r and is small under the influence of B_r.

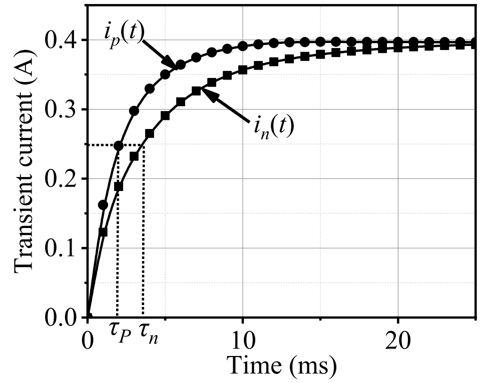

FIGURE 9. The $i_p(t)$ and $i_n(t)$ waveforms when B_t is 0.1T and B_r is 0.83T.

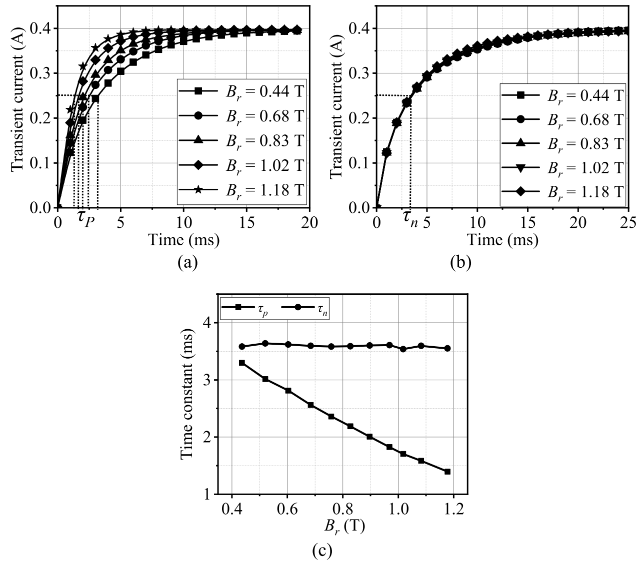

FIGURE 10. The $i_p(t)$ and $i_n(t)$ waveforms and corresponding τ_p and τ_n at different B_r when B_t is 0.10 T and -0.10 T, (a) the $i_p(t)$ waveforms, (b) the $i_n(t)$ waveforms, and (c) the changes of the τ_p and τ_n.

TABLE 3. Time constant value at different residual flux density.

B_r/T	τ_p/ms	τ_n/ms	$\Delta\tau$/ms
0.44	3.30	3.58	0.28
0.52	3.02	3.64	0.62
0.60	2.81	3.62	0.81
0.68	2.56	3.60	1.03
0.76	2.36	3.58	1.22
0.83	2.19	3.59	1.40
0.90	2.01	3.60	1.59
0.97	1.83	3.61	1.78
1.02	1.71	3.54	1.83
1.08	1.59	3.60	2.01
1.18	1.40	3.55	2.16

As shown in Fig. 10, τ_p and τ_n are obtained by the $i_p(t)$ and $i_n(t)$ waveforms at different B_r when B_t is 0.1 T and -0.1 T. And then $\Delta\tau$ is obtained by (1). TABLE 3 shows the value of τ_p, τ_n and $\Delta\tau$ at different B_r when B_t is 0.1 T and -0.1 T.

Through data fitting method, the proposed empirical formula between B_r and $\Delta\tau$ is expressed as

$$B_r = f(\Delta\tau) = a\Delta\tau + b \tag{13}$$

TABLE 4. Fitted parameters valve.

B_t/T	a	b
0.05	0.46	0.44
0.10	0.39	0.29
0.15	0.36	0.20

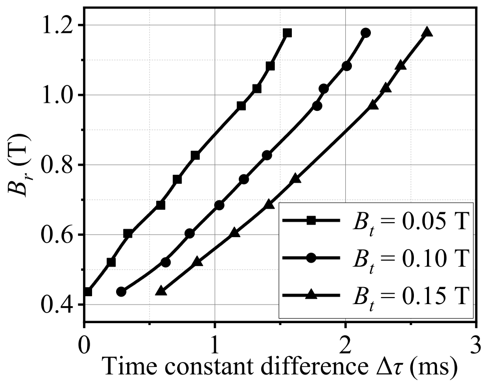

FIGURE 11. The fitting relationship between B_r and $\Delta\tau$ at different B_t.

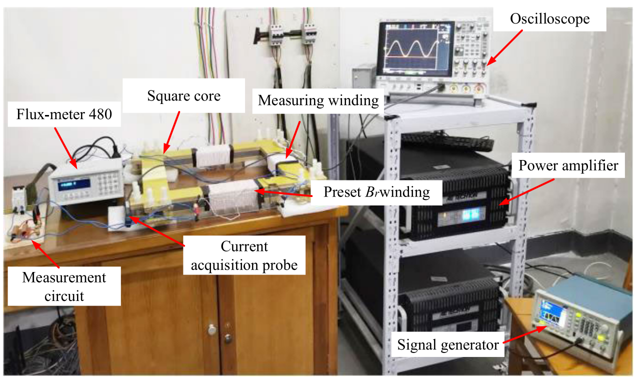

FIGURE 12. The experimental platform of proposed B_r measurement method.

where the parameters a and b are the fitting coefficient, respectively. TABLE 4 shows the parameters a and b at different B_t, and corresponding the relationship between B_r and $\Delta\tau$ is shown in Fig. 11. When B_r in the iron core increases, $\Delta\tau$ increases linearly at different B_t. After that the accuracy of proposed empirical formula will be verified in the experiments in Section IV.

IV. EXPERIMENTAL VALIDATION

A. EXPERIMENTAL PLATFORM

To verify the accuracy of proposed empirical formula, this paper establishes an experimental platform of proposed B_r measurement method, as shown in Fig. 12. The current signal I_m in preset B_r winding and the applied DC voltage $u(t)$ in the measuring winding are respectively obtained by the signal generator. Firstly, a large current signal I_m is applied in the preset B_r winding to generate an initial B_r in the iron core. Then, $u(t)$ is sent through the signal generator, and amplified by the power amplifier, applied in the measuring

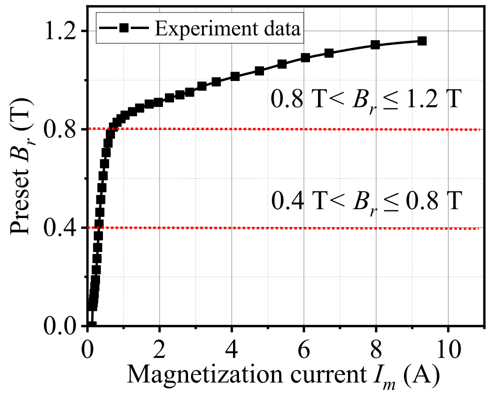

FIGURE 13. The relationship between preset B_r and magnetization current I_m.

winding to result B_t. When B_t is applied, the change of average flux density in the iron core is observed by the Flux-meter 480. Furthermore, the positive and negative transient current waveforms are observed and stored by the oscilloscope. Finally, through the positive and negative transient current waveforms, corresponding τ_p and τ_n are obtained. From this the direction of B_r in the iron core is determined by comparing τ_p and τ_n, and the magnitude of B_r is calculated by proposed empirical formula between B_r and $\Delta\tau$.

B. PRESET RESIDUAL FLUX DENSITY

Fig. 13 shows the relationship between preset B_{rp} and magnetization current I_m. As shown, there is a piecewise linear relationship between preset B_{rp} and I_m. When B_r changes from 0.4 T to 0.8 T, the relationship between preset B_{rp} and corresponding I_m is expressed as:

$$B_{rp} = 5.54I_m^2 + 3.62I_m - 0.48 \tag{14}$$

When B_r changes from 0.8 T to 1.26 T, the relationship between preset B_{rp} and corresponding I_m is expressed as:

$$B_{rp} = 0.05I_m + 0.81 \tag{15}$$

Through (14) and (15), B_r value in the iron core can be predicted more accurately.

C. RESIDUAL FLUX DENSITY MEASUREMENT

Fig. 14 shows the $i_p(t)$ and $i_n(t)$ waveforms when B_r is 0.83 T and B_t is 0.1 T. It can be seen that τ_p and τ_n are obtained by corresponding transient current waveforms. Since the change rate of $i_p(t)$ is greater than that of $i_n(t)$, τ_p is less than τ_n in the transient progress. By comparing τ_p and τ_n, the smaller τ_p is determined as the positive time constant, and the positive direction of B_r is determined. And, the larger τ_n is determined as the negative time constant, and the negative direction of B_r in the iron core is determined. In addition, the simulation results are in good agreement with the measured transient current waveforms. Experimental results prove the accuracy and feasibility of proposed measurement method in FEM.

Fig. 15 shows the $i_p(t)$ and $i_n(t)$ waveforms under different B_r when B_t is 0.1 T and -0.1 T. When preset B_r is 1.18 T,

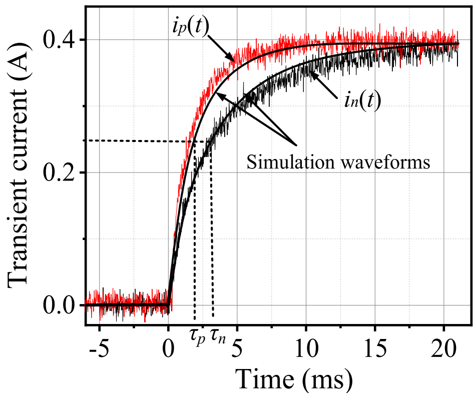

FIGURE 14. The i_p (t) and i_n (t) waveforms when B_r is 0.83T and B_t is 0.1T.

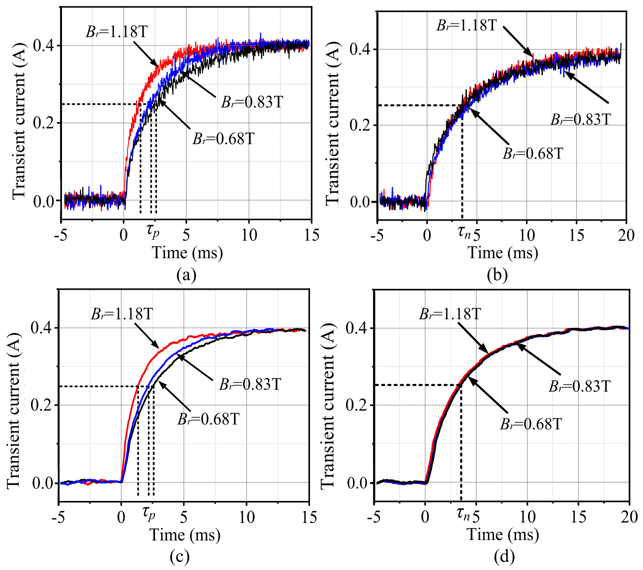

FIGURE 15. The i_p (t) and i_n (t) waveforms at different B_r when B_t is 0.1 T and -0.1 T, (a) measured i_p (t) waveforms, (b) measured i_n (t) waveforms, (c) processed i_p (t) waveforms, and (d) processed i_n (t) waveforms.

0.83 T and 0.68 T, τ_p and τ_n are measured by corresponding transient current waveforms. As shown in Fig. 15(a) and Fig. 15(b), measured $i_p(t)$ and $i_n(t)$ waveforms noise are relatively large. To reduce the measurement error caused by this noise, the moving average method is used to suppress this noise [29]. The processed transient current waveforms are shown in Fig. 15(c) and Fig. 15(d). Through the processed transient current waveforms, τ_p and τ_n are calculated and then corresponding $\Delta\tau$ is substituted into (13) to calculate B_r. The measurement data are shown in TABLE 5. As shown, the preset B_{rp} is obtained by (14) and (15), and the B_{rv} measured in the voltage integration method [21] is obtained by Flux-meter 480. The relative error ε_1 % between B_{rp} and calculated B_r and the relative error ε_2 % between B_{rp} and B_{rv} are expressed as

$$\varepsilon_1\% = \frac{|B_r - B_{rp}|}{B_{rp}} \times 100\% \tag{16}$$

$$\varepsilon_2\% = \frac{|B_{rv} - B_{rp}|}{B_{rp}} \times 100\% \tag{17}$$

TABLE 5. Measurement data.

B_{rp}/T	B_{rv}/T	$\Delta\tau$/ms	B_r/T	ε_1/%	ε_2/%
0.44	0.49	0.44	0.46	4.58	10.85
0.68	0.75	1.08	0.71	4.40	10.22
0.76	0.84	1.12	0.73	4.36	9.98
0.83	0.91	1.29	0.79	4.24	9.85
0.90	0.99	1.47	0.86	4.12	9.52
1.02	1.11	1.77	0.98	4.05	8.89
1.08	1.17	1.91	1.04	4.01	8.43
1.18	1.27	2.16	1.13	3.90	7.75

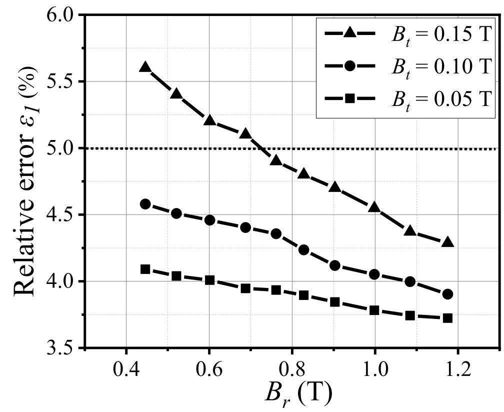

FIGURE 16. The change of ε_1 % at different B_r when B_t is 0.05 T, 0.1 T and 0.15 T.

As shown in TABLE 5, when B_{rp} changes from 0.44 T to 1.18 T, ε_1 % is within 4.58 %, which is less than ε_2 %. Compared with voltage integration method, proposed empirical formula has higher accuracy. Fig. 16 shows the change of ε_1 % when B_t value is 0.05 T, 0.1 T and 0.15 T. In engineering, it is best to control the relative error range within 5 %. When B_t is 0.05 T, the measured transient current signal is weaker so that there is a higher accuracy necessary to the experimental device. And the external electromagnetic interference is large, which is not conducive to signal detection. When B_t is 0.1 T, ε_1 % is within 4.58 %, which meets the requirements of engineering error. When B_t is 0.15 T, the smaller the B_r is, the greater the ε_1 % is. And when B_r is less than about 0.7 T, ε_1 % is greater than 5 %, indicating that the range of measurement B_r is narrow. In summary, when B_t is 0.1 T, the measurement is best in a wide range of B_r in the iron core.

V. CONCLUSION

This paper presents a residual flux density measurement method of the single-phase transformer core based on time constant. Compared with existing residual flux density measurement methods, the main advantages of proposed method include: 1) when the appropriate DC excitation that is the positive or negative direction with residual flux density is applied, the direction of residual flux density is accurately determined by comparing the positive and negative time constant. 2) The magnitude of residual flux density in different directions is calculated by proposed relationship between residual flux density and time constant difference, and its accuracy is verified for a square iron core. When the applied DC voltage is same, the relative error of proposed method is within 4.58 %, which has higher accuracy than voltage integration method. At the same time, it also meets the requirements of engineering error. 3) When an appropriate DC excitation is applied, the magnitude of residual flux density in different ranges is accurately calculated by proposed empirical formula. But the measurement results have higher requirements for the accuracy of measurement instruments. In addition, the proposed measurement method is applicable to transformer cores with different structures which correspond to different empirical formulas. In the future, we hope to analyze different empirical formulas and find the connection between different empirical formulas to solve this problem.

This research provides a reference for selecting the direction and amplitude of demagnetization voltage in the transformer core. In the next step study, the proposed measurement method will be applied to the actual single-phase and three-phase power transformer cores to carry out residual flux density measurement research.

REFERENCES

[1] S. Afrasiabi, M. Afrasiabi, B. Parang, and M. Mohammadi, "Integration of accelerated deep neural network into power transformer differential protection," *IEEE Trans. Ind. Informat.*, vol. 16, no. 2, pp. 865–876, Feb. 2020.

[2] D. Martin, C. Beckett, J. Brown, and S. Nielsen, "Analysis and mitigation of Australian and New Zealand power transformer failures resulting in fires and explosions," *IEEE Elect. Insul. Mag.*, vol. 35, no. 6, pp. 7–14, Nov. 2019.

[3] S. Miyazaki, Y. Mizutani, M. Tahir, and S. Tenbohlen, "Influence of employing different measuring systems on measurement repeatability in frequency response analyses of power transformers," *IEEE Elect. Insul. Mag.*, vol. 35, no. 2, pp. 27–33, Mar. 2019.

[4] F. de Leon, A. Farazmand, S. Jazebi, D. Deswal, and R. Levi, "Elimination of residual flux in transformers by the application of an alternating polarity DC voltage source," *IEEE Trans. Power Del.*, vol. 30, no. 4, pp. 1727–1734, Aug. 2015.

[5] Z. Zhao, X. Li, J. Ji, L. Wei, and T. Wen, "Magnetic characteristics simulation of electrical steel sheet based on Preisach hysteresis model," *High Voltage Technique*, vol. 45, no. 12, pp. 4038–4046, Feb. 2019.

[6] Y. Z. Gerdroodbari, M. Davarpanah, and S. Farhangi, "Remanent flux negative effects on transformer diagnostic test results and a novel approach for its elimination," *IEEE Trans. Power Del.*, vol. 33, no. 6, pp. 2938–2945, Dec. 2018.

[7] Y. Himata, T. Nakajima, T. Koshizuka, M. Saito, and S. Maruyama, "Residual magnetic flux of on-load transformer for controlled switching," *IEEJ Trans. Elect. Electron. Eng.*, vol. 15, no. 8, pp. 1134–1138, 2020.

[8] P. Pachore, Y. Gupta, S. Anand, S. Sarkar, P. Mathur, and P. K. Singh, "Flux error function based controlled switching method for minimizing inrush current in 3-phase transformer," *IEEE Trans. Power Del.*, early access, May 18, 2020, doi: 10.1109/TPWRD.2020.2995519.

[9] W. Ge, J. Zhao, and Y. Wang, "Analysis of the residual flux influence on inrush current and electromagnetic force in large power transformer," *J. Eng.*, vol. 2019, no. 16, pp. 2426–2429, Mar. 2019.

[10] J. Mitra, X. Xu, and M. Benidris, "Reduction of three-phase transformer inrush currents using controlled switching," *IEEE Trans. Ind. Appl.*, vol. 56, no. 1, pp. 890–897, Jan. 2020.

[11] H. Ni, S. Fang, and H. Lin, "A simplified phase-controlled switching strategy for inrush current reduction," *IEEE Trans. Power Del.*, early access, Apr. 2, 2020, doi: 10.1109/TPWRD.2020.2984234.

[12] C. Chen, C. Fang, J. Zeng, W. Li, Y. Luo, and X. Ren, "Research on unloaded transformer controlled switching considering residual flux," *Power Syst. Protection Control*, vol. 46, no. 16, pp. 82–88, Aug. 2018.

[13] S. Fang, H. Ni, H. Lin, and S. L. Ho, "A novel strategy for reducing inrush current of three-phase transformer considering residual flux," *IEEE Trans. Ind. Electron.*, vol. 63, no. 7, pp. 4442–4451, Jul. 2016.

[14] S. Zhang, C. Yao, X. Zhao, J. Li, X. Liu, L. Yu, J. Ma, and S. Dong, "Improved flux-controlled VFCV strategy for eliminating and measuring the residual flux of three-phase transformers," *IEEE Trans. Power Del.*, vol. 35, no. 3, pp. 1237–1248, Jun. 2020.

[15] E. C. G. Santagostino, "Results of the enquiries on actual network conditions when switching magnetizing and small inductive currents and on transformer and shunt reactor saturation characteristics," *Electra*, vol. 94, pp. 35–53, Feb. 1984.

[16] D. Cavallera, V. Oiring, J.-L. Coulomb, O. Chadebec, B. Caillault, and F. Zgainski, "A new method to evaluate residual flux thanks to leakage flux, application to a transformer," *IEEE Trans. Magn.*, vol. 50, no. 2, pp. 1005–1008, Feb. 2014.

[17] Y. Li, M. Jin, H. Li, G. Li, W. Chen, and J. Xie, "Research on measurement method of remanence of power transformer," *Power Syst. Protection Control*, vol. 47, no. 15, pp. 102–107, Aug. 2019.

[18] D. I. Taylor, J. D. Law, B. K. Johnson, and N. Fischer, "Single-phase transformer inrush current reduction using prefluxing," *IEEE Trans. Power Del.*, vol. 27, no. 1, pp. 245–252, Jan. 2012.

[19] S. Zhang, S. Sun, G. Li, K. Wang, J. Li, and J. Liu, "Residual flux characteristics of transformer with single-phase four-limb core under typical condition based on real-time flux tracking," *High Voltage Technique*, early access, pp. 1–11, May 2020, doi: 10.13336/j.1003-6520.hve.20200055.

[20] Z. Shuo, W. Ke, L. Gang, S. Zhang, S. Dong, and C. Yao, "Elimination of residual magnetic flux in power transformers using VFCF strategy," *Electrotech. Appl.*, vol. 39, no. 4, pp. 108–111, Apr. 2020.

[21] T. Liu, X. Liu, S. Liang, J. Wang, and C. Yao, "Residual flux measuring method on the core of ferromagnetic components based on alternating polarity DC voltage source," *Trans. China Electrotech. Soc.*, vol. 32, no. 13, pp. 137–144, Feb. 2017.

[22] Y. Wang, Z. Liu, and H. Chen, "Research on residual flux prediction of the transformer," *IEEE Trans. Magn.*, vol. 53, no. 6, pp. 1–4, Jun. 2017.

[23] W. Yuan, H. Zhang, Y. Shangguan, J. Zou, and J. Yuan, "Analysis on method of calculating transformer residual flux by using the integration of port-voltage waveform and its implementation," in *Proc. 20th Int. Conf. Electr. Mach. Syst. (ICEMS)*, Sydney, NSW, Australia, Aug. 2017, pp. 1–4.

[24] W. Ge, Y. Wang, Z. Zhao, X. Yang, and Y. Li, "Residual flux in the closed magnetic core of a power transformer," *IEEE Trans. Appl. Supercond.*, vol. 24, no. 3, pp. 1–4, Jun. 2014.

[25] C. Huo, Y. Wang, Z. Zhao, and C. Liu, "Residual flux measurement of the single-phase transformer based on transient current method," *IEEE Trans. Appl. Supercond.*, vol. 30, no. 4, pp. 1–5, Jun. 2020.

[26] C. Huo, Y. Wang, S. Wu, Y. Yang, and Z. Zhao, "Residual flux density measurement method for transformer core considering relative differential permeability," *IEEE Trans. Magn.*, early access, Jun. 19, 2020, doi: 10.1109/TMAG.2020.3003658.

[27] W. Q. Ge, Y. H. Wang, X. G. Chen, S. X. Xiao, X. G. Yang, and D. N. Lv, "Method to measure and weaken the residual flux of the power transformer core," *Trans. China Electrotech. Soc.*, vol. 30, no. 16, pp. 10–16, Aug. 2015.

[28] Y.-F. Wu, H.-R. Hu, W. Luo, T. Wang, and L. Ruan, "Research on no-load test of 1000 kV ultra-high voltage transformer," in *Proc. Asia–Pacific Power Energy Eng. Conf.*, Wuhan, China, Mar. 2011, pp. 1–6.

[29] R. Gonzalez and C. A. Catania, "A statistical approach for optimal order adjustment of a moving average filter," in *Proc. IEEE/ION Position, Location Navigat. Symp. (PLANS)*, Monterey, CA, USA, Apr. 2018, pp. 1542–1546.

CAILING HUO was born in Lanzhou, Gansu, China, in 1989. She received the B.E. degree in electrical engineering from Wuhan Textile University, Wuhan, China, in 2012, and the M.E. degree in electrical engineering from Shanghai University of Electric Power, Shanghai, China, in 2015. She is currently pursuing the Ph.D. degree in electrical engineering with the Hebei University of Technology, Tianjin, China. Her currently research interests include measurement on residual flux of power transformer core, and research on inrush current of large power transformer.

SHIPU WU was born in Shijiazhuang, Hebei, China, in 1995. He received the B.E. degree from the Hebei University of Technology, Tianjin, China, in 2017, where he is currently pursuing the Ph.D. degree in electrical engineering. His currently research interests include measurement on residual flux of power transformer core, and research on inrush current of large power transformer

YIMING YANG was born in Xingtai, Hebei, China, in 1995. He received the B.E. degree in electrical engineering from the China University of Mining and Technology, Xuzhou, China, in 2018. He is currently pursuing the M.E. degree in electrical engineering with the Hebei University of Technology, Tianjin, China. His research interest includes study on loss separation of soft magnetic composites the design.

CHENGCHENG LIU (Member, IEEE) was born in Jiangsu, China, in 1988. He received the B.E. degree in automation engineering from Yangzhou University, Yangzhou, China, in 2010, and the Ph.D. degree in electrical engineering from the Hebei University of Technology, Tianjin, China, in 2016. He was the joint Ph.D. student supported by the Chinese scholarship council with the University of Technology, Sydney, NSW, Australia. He is currently a Lecturer with the Hebei University of Technology. His research interests include the design, analysis, control, and optimization of electromagnetic devices.

YOUHUA WANG was born in Jiujiang, Jiangxi, China, in 1964. He received the B.E. degree from Xian Jiaotong University, Xian, China, in 1987, the M.E. degree from the Hebei University of Technology, Tianjin, China, in 1990, and the Ph.D. from Fuzhou University, Fuzhou, China, in 1994, all in electrical apparatus. He is currently a Professor with the College of Electrical Engineering. His currently research interests include measurement and modeling of properties of magnetic materials, numerical analysis of the electromagnetic field, and electromagnetic device design, analysis, and optimization.